



Cite this: *Photochem. Photobiol. Sci.*, 2019, **18**, 2782

Received 2nd June 2019,  
Accepted 30th September 2019

DOI: 10.1039/c9pp00254e

rsc.li/pps

## Homogeneous photochemical water oxidation with metal salophen complexes in neutral media†

Md. Ali Asraf,<sup>a,b</sup> Chizoba I. Ezugwu,<sup>a</sup> C. M. Zakaria<sup>b</sup> and Francis Verpoort  <sup>a,c,d</sup>

The development of water oxidation catalysts based on Earth-abundant metals that can function at neutral pH remains a basic chemical challenge. Here, we report that salophen complexes with Ni(II), Cu(II), and Mn(II) can catalyse photochemical water oxidation to molecular oxygen in the presence of [Ru(bpy)<sub>3</sub>]<sup>2+</sup> as a photosensitizer and Na<sub>2</sub>S<sub>2</sub>O<sub>8</sub> as an oxidant in phosphate buffer of pH 7.0. Experimental results including CV, SEM, EDS, ESI-MS, and DLS measurements on the metal salophen complex-catalysed water oxidation to oxygen suggest that the catalytic activity of the catalysts is molecular in origin.

### Introduction

Solar energy is employed with excellent efficiency to provide high-energy chemicals such as sugar by photosynthesis, during which nature's cuboidal CaMn<sub>4</sub>O<sub>5</sub> oxygen-evolving complex (OEC) of photosystem II (PSII) oxidizes H<sub>2</sub>O to extract protons and electrons.<sup>1–6</sup> In order to mimic the function and structure of the OEC CaMn<sub>4</sub>O<sub>5</sub> in PSII, scientists have made considerable efforts towards the development of the model complexes of PSII for water oxidation.<sup>7–12</sup> For instance, numerous manganese complexes have been examined for the oxidation of water.<sup>7,13–16</sup> Additionally, a series of complexes and oxides of Ru and Ir have been studied as WOCs, since the late 1970s.<sup>17–23</sup> Nevertheless, because of the low abundance and high price of these noble metals, limitations might arise for the application of these catalysts in establishing an artificial photosynthetic system.<sup>1</sup> As a consequence, water oxidation catalysts with low overpotential and high efficiency, made of cheap and abundant metals, are extremely desirable.<sup>24–28</sup> In recent years, catalysts (homogeneous and heterogeneous) based on first-row transition metals have attracted a lot of attention for the oxidation of water.<sup>29–62</sup> Salophen and Salen Schiff bases can be synthesized by the condensation of amines and aldehydes under different reaction conditions.<sup>63</sup> They are

capable of stabilizing metals in different oxidation states in four coordination geometries and controlling the activity of metals in a large diversity of productive catalytic transformations.<sup>64</sup> Schiff base metal complexes are of enormous importance for catalysis.<sup>65</sup> More recently, it is reported that cobalt salophen and salen complexes can act as homogeneous or heterogeneous catalysts for the oxidation of water, depending on the reaction conditions.<sup>29,38,66</sup> Inspired by these reports, we decided to check the water oxidation activity of other metal salophen complexes such as copper salophen, nickel salophen, and manganese salophen. From the literature, it is found that most of the water oxidation catalysts operate under acidic or basic conditions, whereas only few operate at neutral pH.<sup>67–72</sup> The development of WOCs made of Earth-abundant, first-row metals that operate under neutral conditions remains a basic challenge. Herein, we report that metal [Cu(II), Ni(II) and Mn(II)] salophen complexes act as stable catalysts in photochemical water oxidation in the presence of Ru(bpy)<sub>3</sub><sup>2+</sup> as the photosensitizer and S<sub>2</sub>O<sub>8</sub><sup>2-</sup> ions as sacrificial electron acceptors at neutral pH.

### Experimental section

#### Materials

All chemical reagents, including *o*-phenylenediamine (99.0%), salicylaldehyde (98.0%), copper acetate monohydrate (Cu(OAc)<sub>2</sub>·H<sub>2</sub>O; 99.5%), nickel acetate tetrahydrate (Ni(OAc)<sub>2</sub>·4H<sub>2</sub>O; 98.0%), manganese acetate tetrahydrate (Mn(OAc)<sub>2</sub>·4H<sub>2</sub>O; 98.0%), tris(2,2'-bipyridyl)dichlororuthenium(II) hexahydrate ([Ru(bpy)<sub>3</sub>]Cl<sub>2</sub>·6H<sub>2</sub>O; 99.95%), sodium persulfate (Na<sub>2</sub>S<sub>2</sub>O<sub>8</sub>; 99.99%), sodium dihydrogen phosphate anhydrous (NaH<sub>2</sub>PO<sub>4</sub>; 99.0%), sodium phosphate dibasic (Na<sub>2</sub>HPO<sub>4</sub>; 99.0%), sodium hydroxide (NaOH; 96.0%), ethanol (EtOH; 99.7%), and methanol (MeOH; 99.5%), were purchased from Aldrich or

<sup>a</sup>Laboratory of Organometallics, Catalysis and Ordered Materials, State Key Laboratory of Advanced Technology for Materials Synthesis and Processing, Wuhan University of Technology, Wuhan 430070, China.

E-mail: Francis.Verpoort@ghent.ac.kr; Fax: +862787879468; Tel: +8615071172245

<sup>b</sup>Department of Chemistry, Rajshahi University, Rajshahi-6205, Bangladesh

<sup>c</sup>National Research Tomsk Polytechnic University, Lenin Avenue 30, 634050 Tomsk, Russian Federation

<sup>d</sup>Ghent University, Global Campus Songdo, 119 Songdomunhwa-Ro, Yeonsu-Gu, Incheon, Korea

† Electronic supplementary information (ESI) available: Characterization studies (<sup>1</sup>H and <sup>13</sup>C NMR). See DOI: 10.1039/c9pp00254e

Across. All chemicals and solvents were used as received. Purified water obtained from Milli-Q system (resistivity:  $\sim 18$  MQ cm) was used for the preparation of aqueous solutions.

### Spectroscopic measurements

$^1\text{H}$  and  $^{13}\text{C}$  NMR spectra were recorded with a Bruker 500 MHz NMR spectrometer using TMS as the internal standard and  $[\text{d}_6]$  DMSO as the solvent. ESI-MS spectra were performed using an Agilent Technologies MSD SL Trap mass spectrometer with an ESI source coupled with an 1100 Series HPLC system. FT-IR spectra were recorded using a Nicolet 5700 FT-IR instrument. DLS (dynamic light scattering) measurements were performed using a Zetasizer Nano ZS; Malvern Instruments (particle size distribution from 0.6 to 6000 nm and detection limit of 0.1 ppm) for all the reaction solutions.

### Elemental analysis

Elemental analyses for CHNO were performed using a Vario EL cube [Elements (Elemental) analysis system, Germany].

### Electrochemical measurements

Cyclic voltammetry experiments were carried out using a CHI660E Electrochemical Analyzer Series/Workstation. A standard three-electrode electrochemical cell consisting of a glassy carbon electrode (working electrode), Ag/AgCl (reference electrode) and a Pt wire (auxiliary electrode) was used. All the cyclic voltammetry experiments were carried out with a scanning rate of  $100 \text{ mV s}^{-1}$ . Prior to electrochemical measurements, the glassy carbon electrode was polished with 0.3, 0.1, and  $0.05 \mu\text{m}$  of alumina slurry for 5 min each to get a mirror surface, followed by ultrasonication in ethanol and Millipore water, respectively, at least two times (3–5 min).

### Photochemical water oxidation and oxygen evolution quantified by GC

Photochemical water oxidation experiments were performed as follows: A salophen complex (1–50  $\mu\text{M}$ ) was added to a phosphate buffer (0.1 M, pH 7.0, 5.0 mL) containing  $[\text{Ru}(\text{bpy})_3]\text{Cl}_2 \cdot 6\text{H}_2\text{O}$  (1.0 mM) and  $\text{Na}_2\text{S}_2\text{O}_8$  (5.0 mM) deaerated by purging with  $\text{N}_2$  gas for 30 min in a 34 mL flask sealed with a rubber septum. The water oxidation reaction was carried out by irradiating the solution with a 500 W Xe-lamp through a transmitting glass filter ( $\lambda \geq 420 \text{ nm}$ ) at room temperature. After each sampling time, 100  $\mu\text{L}$  of  $\text{N}_2$  was injected into the flask and then 100  $\mu\text{L}$  of the gas sample was withdrawn using a SGE gas-tight syringe and analysed by a gas chromatographer (GC) equipped with a thermal conductive detector and 5 Å molecular sieve column (2 mm  $\times$  3 mm) and with He as a carrier gas. The total amount of evolved  $\text{O}_2$  was calculated based on the concentration of  $\text{O}_2$  in the headspace gas. The pH of the reaction solution was monitored after the water oxidation reaction using a Sartorius PB-10 pH meter.

### Electron microscopy measurements

The sample for SEM measurements was prepared from the bulk electrolysis of a solution of 0.5 mM catalyst in 0.1 M phos-

phate buffer of pH 7.0 using a glassy carbon electrode. The electrolysis was carried out for 2 h under rapid (400 rpm) stirring at 1.2 V. After 2 h of bulk electrolysis, the glassy carbon electrode was taken out and gently rinsed with Millipore water, air dried, and then dried under vacuum. Field-Emission Scanning Electron Microscopy (FE-SEM) images and SEM-EDX data were obtained using a ZEISS ULTRA PLUS-43-13 on connection to an Energy-Dispersive Spectrometer (OXFORD X-Max 50). The acceleration voltage was 15 kV.

### Synthesis of the salophen ligand (Slp)

The ligand, salophen was prepared according to the reported procedure.<sup>73</sup> 1 mM *o*-phenylenediamine solution in ethanol was added dropwise to the 2 mM solution of salicylaldehyde in ethanol and then the mixture of the solutions was refluxed for 2 h at 85 °C. The precipitated Schiff-base ligand was filtered, washed with cold ethanol and finally recrystallized from hot ethanol giving the desired product, **Slp**.

### Salophen ligand (Slp)

Orange crystals; yield 90%;  $^1\text{H NMR}$  ( $[\text{d}_6]$ DMSO): 12.94 (s, 2H), 8.93 (s, 2H), 7.66 (dd, 2H), 6.93–7.50 (m, 10H).  $^{13}\text{C NMR}$  ( $[\text{d}_6]$ DMSO): 164.53 (C–OH), 160.96 (C=N), 142.85, 133.92, 132.90, 128.31, 120.23, 119.97, 119.56, 117.09 (all are Ar.C). **FT-IR** (**KBr**,  $\text{cm}^{-1}$ ): 3203–2400 (m, OH), 3051 (w, aromatic C–H), 1610 (s, C=N), 1190 (phenolic C–O). **Elemental Analysis**: Calculated: C, 75.93; H, 5.10; N, 8.86; O, 10.11%. Found: C, 76.04; H, 5.24; N, 8.90; O, 9.82%.

### Preparation of the salophen Ni(II) complex, 1

The salophen Ni(II) complex was prepared as follows: 2 mM solution of  $\text{Ni}(\text{OAc})_2 \cdot 4\text{H}_2\text{O}$  and 2 mM solution of the salophen ligand in 50 mL of ethanol were refluxed with vigorous stirring for 2 h. The reaction progress was monitored by TLC. The reaction mixture was then cooled to room temperature and the obtained solid product was filtered, washed with cold EtOH and  $\text{Et}_2\text{O}$ , and dried.<sup>74,75</sup>

### Salophen Ni(II) complex, 1

Yield 83%;  $^1\text{H NMR}$  ( $[\text{d}_6]$ DMSO): 8.91 (s, 2H), 8.16 (q, 2H), 7.62 (dd, 2H), 7.37 (m, 2H), 7.32 (m, 2H), 6.90 (d, 2H), 6.68 (t, 2H).  $^{13}\text{C NMR}$  ( $[\text{d}_6]$ DMSO): 165.70 (C=N), 157.08 (C–O), 142.97, 135.66, 134.87, 128.08, 120.77, 116.59, 115.80, 100.17 (all are Ar.C). **FT-IR** (**KBr**,  $\text{cm}^{-1}$ ): 3063 (w, aromatic C–H), 1601 (s, C=N), 1194 (phenolic C–O). **ESI-MS** ( $\text{H}_2\text{O}$ ,  $m/z$ ): 372.1656  $[\{\text{Ni}(\text{C}_{20}\text{H}_{14}\text{N}_2\text{O}_2)\text{H}\}]^+$ . **Elemental Analysis**: Calculated: C, 64.40; H, 3.78; N, 7.51; O, 8.58%. Found: C, 64.62; H, 3.82; N, 7.53; O, 8.64%.

### Synthesis of the salophen Cu(II) complex, 2

0.5 mM solution of the salophen ligand in ethanol (10 mL) and 0.5 mM solution of  $\text{Cu}(\text{OAc})_2 \cdot \text{H}_2\text{O}$  in water (1 mL) were mixed and refluxed with vigorous stirring for 3 h. The solution mixture was then cooled to room temperature and filtered. After filtration, the obtained solid product was washed

thoroughly with water, ethanol and diethyl ether, then dried *in vacuo* to afford the desired product.<sup>76</sup>

### Salophen Cu(II) complex, 2

Yield 74%; FT-IR (KBr,  $\text{cm}^{-1}$ ): 3065 (w, aromatic C-H), 1600 (s, C=N), 1195 (phenolic C-O). ESI-MS ( $\text{H}_2\text{O}$ ,  $m/z$ ): 377.0716  $[\{\text{Cu}(\text{C}_{20}\text{H}_{14}\text{N}_2\text{O}_2)\}_2\text{H}]^+$ . Elemental Analysis: Calculated: C, 63.57; H, 3.73; N, 7.41; O, 8.47%. Found: C, 63.65; H, 3.78; N, 7.44; O, 8.52%.

### Synthesis of the salophen Mn(II) complex, 3

Owing to its air sensitivity, the salophen Mn(II) complex was synthesized under argon with strict exclusion of air. To a 4 mM solution of the salophen ligand in 40 mL of deaerated absolute EtOH was added an 8 mM solution of KOH dissolved in 10 mL of deaerated absolute EtOH through a cannula needle. To this resulting solution was added dropwise a 4 mM solution of  $\text{Mn}(\text{OAc})_2 \cdot 4\text{H}_2\text{O}$  in 10 mL of deaerated absolute EtOH using a Teflon cannula. The solution mixture was stirred vigorously for 1.5 h at room temperature and refluxed for 5 h at 90 °C. The solution mixture was then cooled to room temperature and the obtained yellow product was filtered, washed with deaerated EtOH and dried *in vacuo*.<sup>77</sup>

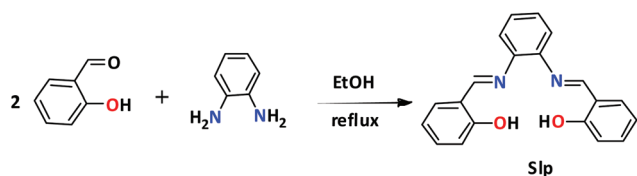
### Salophen Mn(II) complex, 3

Yield 68%; FT-IR (KBr,  $\text{cm}^{-1}$ ): 3057 (w, aromatic C-H), 1606 (s, C=N), 1197 (phenolic C-O). ESI-MS ( $\text{H}_2\text{O}$ ,  $m/z$ ): 369.0103  $[\{\text{Mn}(\text{C}_{20}\text{H}_{14}\text{N}_2\text{O}_2)\}_2\text{H}]^+$ . Elemental Analysis: Calculated: C, 65.05; H, 3.82; N, 7.59; O, 8.67%. Found: C, 65.11; H, 3.88; N, 7.62; O, 8.73%.

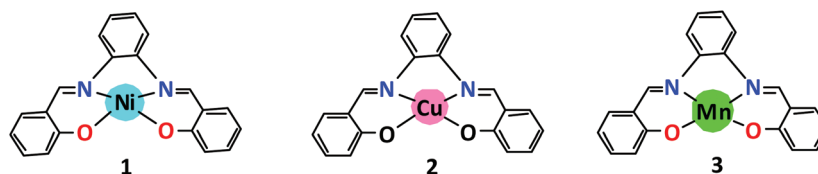
## Results and discussion

### Structural characterization studies of the ligand and catalysts

The ligand, **Slp** (Scheme 1), and the complexes 1–3 (Scheme 2) were prepared and characterized by elemental analysis,  $^1\text{H}$  and



Scheme 1 Preparation of the Schiff base ligand, salophen (Slp).



Scheme 2 Structure of the complexes studied in this work.

$^{13}\text{C}$  NMR spectroscopy, FT-IR spectroscopy, and ESI-MS spectroscopy.

$^1\text{H}$  and  $^{13}\text{C}$  NMR spectra (Fig. S1 and S2†) of the prepared ligand confirm the formation of the ligand.  $^1\text{H}$  NMR spectrum of the ligand, **Slp**, shows the OH proton and imine proton features at 12.94 and 8.93 ppm, respectively.  $^{13}\text{C}$  NMR spectra also support the proposed structure of the ligand, showing the signals at 164.53 ppm (C–OH) and at 160.96 ppm (C=N). The OH proton peak in the  $^1\text{H}$  NMR spectra of the free ligand disappears in the case of complex **1**, confirming that the OH group of the ligand has been deprotonated and coordinated to the metal, nickel (Fig. S4†). The imine proton signal (8.93 ppm) in the  $^1\text{H}$  NMR spectra of the free ligand has been shifted to higher field (8.88 ppm). Moreover, the  $^{13}\text{C}$  NMR spectra of complex **1** also support the proposed structure (Fig. S5†). Furthermore, it is important to mention that in the tetracoordinated Ni(II) complex, the electronic magnetic field shortens the nuclear longitudinal relaxation times of the nuclei less effectively, thus sharpening the broad peaks typically associated with paramagnetic substances. Tetracoordinated Ni(II) with 3-fold orbitally degenerate ground states often has short electron–spin lifetimes that permit well-resolved NMR signals.<sup>78–80</sup> In this case, hyperfine shifts are concerned, the larger magnetic anisotropy induces large dipolar contributions; negligible in the case of octahedral Ni(II).<sup>81–83</sup> The FT-IR spectra of the ligand and complexes (Fig. S3 and S6–S8†) confirm the formation of the ligand and complexes with the proposed structures (Scheme 2). By complexation, the broad O–H absorption bands of the salophen ligand in the region from 3203 to 2240  $\text{cm}^{-1}$  are absent in the FT-IR spectra of the complexes 1–3, confirming that the salophen ligand is deprotonated in the complexation and the oxygens are coordinated to the metal atom. In addition, the IR spectra of 1–3, compared with the ligand, indicate that the  $\nu(\text{C}=\text{N})$  stretching band at 1610  $\text{cm}^{-1}$  is shifted to lower energy by 4–10  $\text{cm}^{-1}$  for salophen complexes, confirming that the ligand **Slp** is coordinated to the metal ions through nitrogen atoms of the azomethine groups. The electrospray mass spectrum of the salophen complexes (Fig. 1) also supports the proposed structure of the complexes, showing ions at mass-to-charge ratio ( $m/z$ ) of 372.1656, 377.0716, and 369.0103 matching the calculated values for the ions  $[\{\text{Ni}(\text{C}_{20}\text{H}_{14}\text{N}_2\text{O}_2)\}_2\text{H}]^+$ ,  $[\{\text{Cu}(\text{C}_{20}\text{H}_{14}\text{N}_2\text{O}_2)\}_2\text{H}]^+$  and  $[\{\text{Mn}(\text{C}_{20}\text{H}_{14}\text{N}_2\text{O}_2)\}_2\text{H}]^+$ , respectively.

### Electrochemical studies

Cyclic voltammograms of three different water-soluble complexes, 1–3, in 0.1 M NaPi buffer of pH 7.0 were obtained on a

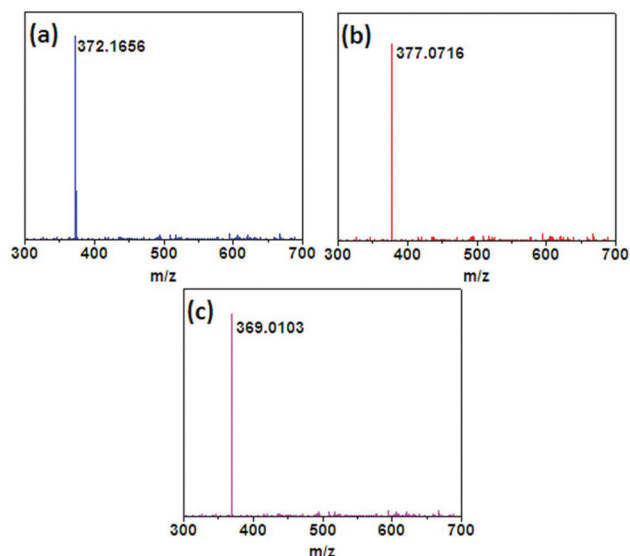


Fig. 1 ESI-MS spectra of a  $10^{-5}$  M solution of (a) **1**, (b) **2**, and (c) **3** in  $\text{H}_2\text{O}$ .

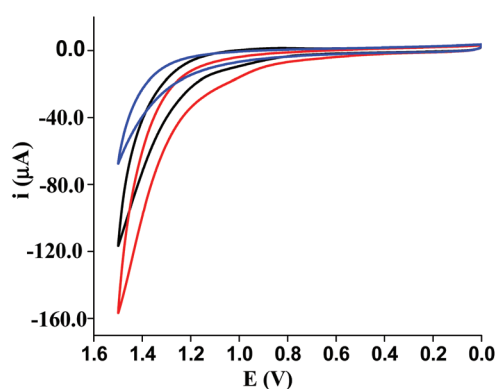
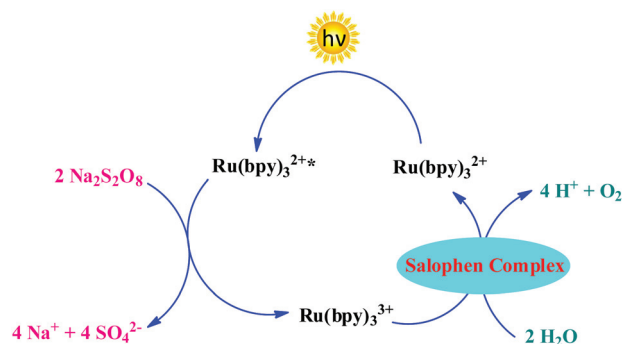


Fig. 2 Cyclic voltammograms of 0.5 mM **1** (black), **2** (red), and **3** (blue) recorded in 0.1 M phosphate buffer of pH 7.0 using a glassy carbon as the working electrode, Ag/AgCl as the reference electrode and a Pt wire as the auxiliary electrode at a scan rate of  $100 \text{ mV s}^{-1}$  at 1.5 V.

glassy carbon electrode (Fig. 2). Potentials were measured *vs.* an Ag/AgCl reference electrode. The CVs of all three complexes exhibited large, irreversible oxidation waves on scanning at  $100 \text{ mV s}^{-1}$  from 0 to +1.5 V that correspond to the catalytic oxidation of  $\text{H}_2\text{O}$  to  $\text{O}_2$ . The onset potential for the catalytic oxidation of  $\text{H}_2\text{O}$  for all the catalysts ranges from 0.98 to 1.16 V (*vs.* Ag/AgCl). The peak currents were  $116 \mu\text{A}$ ,  $157 \mu\text{A}$ , and  $67 \mu\text{A}$  at  $100 \text{ mV s}^{-1}$  using a  $0.07 \text{ cm}^2$  glassy carbon electrode for the complexes **1**, **2**, and **3**, respectively.

### Visible light-driven water oxidation

The catalytic activity of the complexes **1–3** for photochemical water oxidation was investigated using  $[\text{Ru}(\text{bpy})_3]\text{Cl}_2 \cdot 6\text{H}_2\text{O}$  as the photosensitizer and  $\text{S}_2\text{O}_8^{2-}$  as the sacrificial electron acceptor, at pH 7.0 in 0.1 M phosphate buffer. The catalytic cycle of the photochemical water oxidation is shown in



Scheme 3 Catalytic cycle of visible light-driven water oxidation with the  $[\text{Ru}(\text{bpy})_3]^{2+}/\text{S}_2\text{O}_8^{2-}$  system catalysed by the salophen complex.

Scheme 3. Photoinduced electron transfer from  $[\text{Ru}(\text{bpy})_3]^{2+*}$  (where \* denotes the excited state) to  $\text{Na}_2\text{S}_2\text{O}_8$  affords  $[\text{Ru}(\text{bpy})_3]^{3+}$ , which can oxidize  $\text{H}_2\text{O}$  to  $\text{O}_2$  in the presence of water oxidation catalysts.

Visible light-driven water oxidation experiments were carried out as follows: A salophen complex (1–50  $\mu\text{M}$ ) was added to a phosphate buffer (0.1 M, pH 7.0, 5.0 mL) containing  $[\text{Ru}(\text{bpy})_3]\text{Cl}_2 \cdot 6\text{H}_2\text{O}$  (1.0 mM) and  $\text{Na}_2\text{S}_2\text{O}_8$  (5.0 mM) deaerated by purging with  $\text{N}_2$  gas for 30 min in a 34 mL flask sealed with a rubber septum. The water oxidation reaction was carried out by irradiating the solution with a 500 W Xe-lamp through a transmitting glass filter ( $\lambda \geq 420 \text{ nm}$ ) at room temperature. After each sampling time, 100  $\mu\text{L}$  of  $\text{N}_2$  was injected into the flask and then 100  $\mu\text{L}$  of the gas sample was withdrawn using a SGE gas-tight syringe and analysed by a gas chromatographer (GC) equipped with a thermal conductive detector and 5  $\text{\AA}$  molecular sieve column (2 mm  $\times$  3 mm) and with He as a carrier gas. The total amount of evolved  $\text{O}_2$  was calculated based on the concentration of  $\text{O}_2$  in the headspace gas. The pH of the reaction solution was monitored after the water oxidation reaction using a Sartorius PB-10 pH meter.

The maximum turnover numbers and the total quantity of  $\text{O}_2$  formed in the photocatalytic system depend on the concentration of the catalyst (Fig. 3). Both increased with an increase in catalyst concentration, indicating single-site water oxidation catalysis.

The water oxidation reaction catalyzed by the complex **2** under different concentrations of the photosensitizer,  $[\text{Ru}(\text{bpy})_3]^{2+}$ , and the sacrificial electron acceptor,  $\text{Na}_2\text{S}_2\text{O}_8$ , was performed (Fig. 4 and 5). The  $\text{O}_2$  yield increased when the concentration of the photosensitizer increased from 0.4 to 1.0 mM. Nonetheless, the  $\text{O}_2$  yield started to decrease with increasing the concentration of the photosensitizer above 1.0 mM (for example, 1.5 mM) (Fig. 4). We also examined the concentration effect of the oxidant  $\text{Na}_2\text{S}_2\text{O}_8$  on the quantity of  $\text{O}_2$  formed in the water oxidation reaction catalyzed by the complex **2** (Fig. 5). The amount of produced  $\text{O}_2$  increased with an increasing concentration of the oxidant up to 5 mM, but decreased when the concentration of the oxidant was more than 5 mM. The observed results at 1.5 mM concentration of  $[\text{Ru}(\text{bpy})_3]^{2+}$  and 7.0 mM  $\text{Na}_2\text{S}_2\text{O}_8$  can be attributed to non- $\text{O}_2$

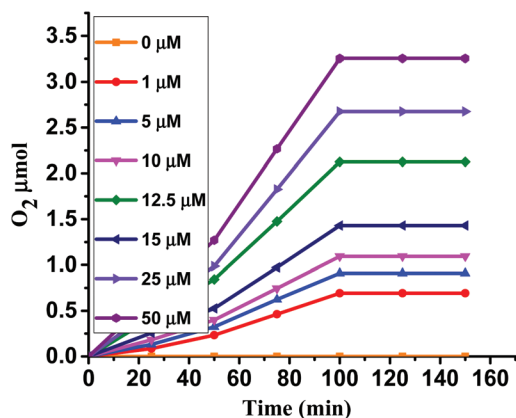


Fig. 3  $O_2$  evolution kinetics in the photoactivated system,  $[2] = 1\text{--}50\ \mu\text{M}$ ,  $[\text{Ru}(\text{bpy})_3]^{2+} = 1.0\ \text{mM}$ ,  $[\text{S}_2\text{O}_8^{2-}] = 5.0\ \text{mM}$  in  $0.1\ \text{M}$  NaPi buffer,  $\text{pH} = 7.0$ ; illumination using a  $500\ \text{W}$  Xe-lamp ( $\lambda \geq 420\ \text{nm}$ ).

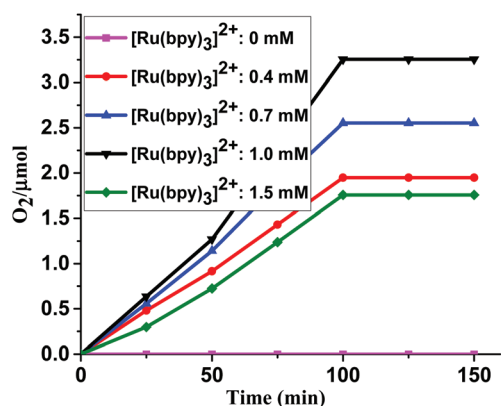


Fig. 4 Kinetics of  $O_2$  formation under photoirradiation [ $500\ \text{W}$  Xe-lamp ( $\lambda \geq 420\ \text{nm}$ )] of a phosphate buffer solution ( $0.1\ \text{M}$ ,  $\text{pH}\ 7.0$ ,  $5.0\ \text{mL}$ ) containing  $5.0\ \text{mM}$   $[\text{S}_2\text{O}_8^{2-}]$  and  $50\ \mu\text{M}$  complex 2 using different concentrations of the photosensitizer,  $[\text{Ru}(\text{bpy})_3]^{2+}$  ( $1.0\ \text{mM}$ , black;  $0.7\ \text{mM}$ , blue;  $0.4\ \text{mM}$ , red;  $1.5\ \text{mM}$ , olive).

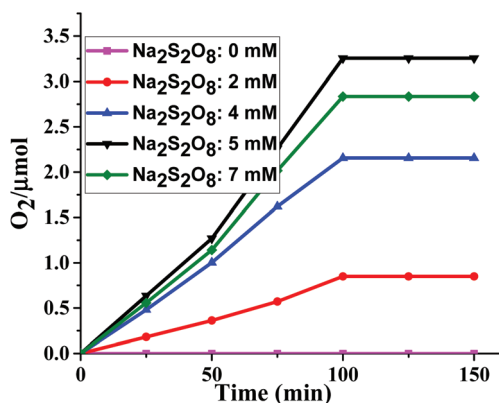


Fig. 5 Kinetics of  $O_2$  formation under photoirradiation [ $500\ \text{W}$  Xe-lamp ( $\lambda \geq 420\ \text{nm}$ )] of a phosphate buffer solution ( $0.1\ \text{M}$ ,  $\text{pH}\ 7.0$ ,  $5.0\ \text{mL}$ ) containing  $1.0\ \text{mM}$   $[\text{Ru}(\text{bpy})_3]^{2+}$  and  $50\ \mu\text{M}$  complex 2 using different concentrations of  $\text{Na}_2\text{S}_2\text{O}_8$  ( $5.0\ \text{mM}$ , black;  $7.0\ \text{mM}$ , olive;  $4.0\ \text{mM}$ , blue;  $2.0\ \text{mM}$ , red).

productive decomposition reactions between  $\text{Na}_2\text{S}_2\text{O}_8$  and  $[\text{Ru}(\text{bpy})_3]^{2+}$ .<sup>32,84,85</sup> Thus, the optimal concentrations of the photosensitizer and the sacrificial electron acceptor for the water oxidation reaction were  $1\ \text{mM}$  and  $5\ \text{mM}$ , respectively. There was no  $O_2$  formation in the absence of the photosensitizer,  $[\text{Ru}(\text{bpy})_3]^{2+}$ , and the sacrificial electron acceptor,  $\text{Na}_2\text{S}_2\text{O}_8$ .<sup>61</sup>

Maximum  $O_2$  formation amounts of  $3.25$ ,  $2.50$ , and  $1.0\ \mu\text{mol}$  were obtained from  $50\ \mu\text{M}$  **1**, **2**, and **3**, respectively, in  $0.1\ \text{M}$  NaPi buffer of  $\text{pH}\ 7.0$  after  $2.5\ \text{h}$  of photocatalysis (Fig. 6). The low oxygen yields at a lower catalyst concentration are probably because the diffusion-controlled interactions between the catalyst and photosensitizer were not sufficient.<sup>86</sup> The  $O_2$  evolution kinetics of the photoactivated system catalyzed by complexes **1** and **2** showed a short induction period and is possibly due to a slow solution-to-gas transfer of the  $O_2$  or a slow mass transfer of  $O_2$  into a head-space.<sup>87,88</sup> The initial sluggish kinetics of the  $O_2$  evolution reaction may also be observed if initially not enough amount of reactive metal-oxo or -hydroperoxidic intermediates<sup>34,89–94</sup> was generated during the reaction between  $\text{Ru}(\text{III})$  and metal-salophen complexes. The  $O_2$  evolution during the photochemical water oxidation reaction using metal-salophen complexes showed saturation at  $\sim 100$  minutes and the  $\text{pH}$  of the resulting solution dropped from  $7.0$  to  $6.74$ . The saturation observed for the  $O_2$  evolution and a decrease in the  $\text{pH}$  of the solution were probably due to proton accumulation in the reaction mixture, which is attributed to most proton-coupled electron transfer (PCET) processes.<sup>71,95</sup> PCET pathways produce reactive  $\text{M}=\text{O}$  intermediates ( $\text{M} = \text{metal}$ ), which are primed to form an  $\text{O}-\text{O}$  bond with either a water molecule or another catalyst molecule.<sup>96</sup> The complex **2** showed a high activity with a turnover number of  $13$  for  $O_2$  evolution, whereas the complexes **1** and **3** exhibited water oxidation activity with turnover numbers of  $10$  and  $4$ , respectively.

### The identity of the true catalyst

To examine the nature of true catalytic materials in the water oxidation reaction by **1**, **2**, and **3** under neutral conditions, we

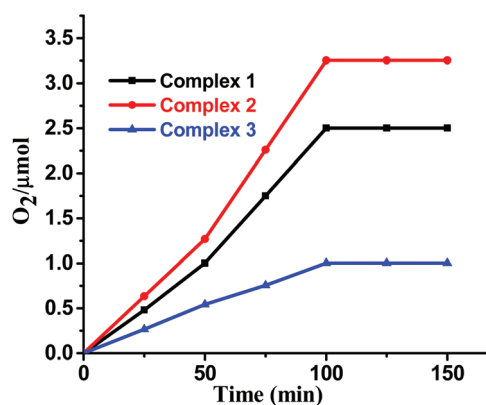
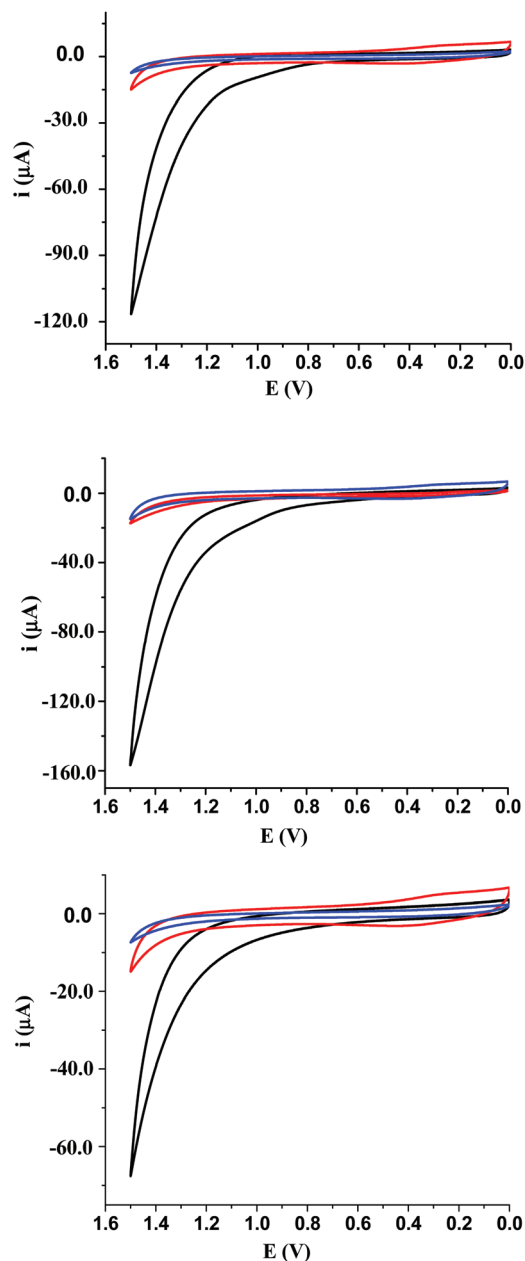
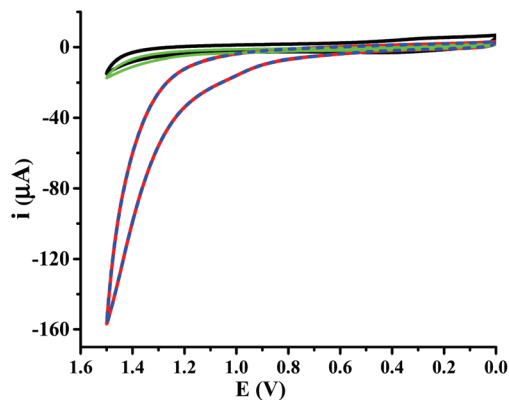


Fig. 6 Time courses of oxygen evolution under photoirradiation [ $500\ \text{W}$  Xe-lamp ( $\lambda \geq 420\ \text{nm}$ )] of a phosphate buffer solution ( $0.1\ \text{M}$ ,  $\text{pH}\ 7.0$ ,  $5.0\ \text{mL}$ ) containing  $1.0\ \text{mM}$   $[\text{Ru}(\text{bpy})_3]^{2+}$ ,  $5.0\ \text{mM}$   $[\text{S}_2\text{O}_8^{2-}]$ , and  $50\ \mu\text{M}$  catalyst.

performed 20 CV scans of 0.5 mM complexes **1**, **2**, and **3** in 0.1 M NaPi buffer of pH 7.0 at a glassy carbon electrode. The working electrode was thoroughly rinsed with water after the above CV scans, but not polished, and then the electrode was cycled in a fresh catalyst free 0.1 M NaPi buffer of pH 7.0. No considerable catalytic current was produced relative to a freshly polished electrode (Fig. 7), indicating that the electrocatalysis of **1**, **2**, and **3** did not lead to any catalytic film depo-



**Fig. 7** Cyclic voltammograms of 0.5 mM **1** (top), **2** (middle), and **3** (bottom). Black: CV using catalysts. Red: CV of the fresh buffer solution using an unpolished glassy carbon electrode. Blue: CV of the fresh buffer solution using a freshly polished working electrode. Phosphate buffer concentration and pH: 0.1 M and 7.0, potential: 0–1.5 V vs. Ag/AgCl and scan rate: 100 mV s<sup>-1</sup>.



**Fig. 8** Cyclic voltammograms of 0.1 M phosphate buffer of pH 7.0 without any catalyst (black solid line), with 1 mM Cu<sup>2+</sup> in 0.1 M phosphate buffer (green solid line), with 0.5 mM complex **2** in 0.1 M phosphate buffer (red solid line), and with 2,2'-bipyridine (bpy) (after several CV scans with the complex **2**, excess bpy is added to the solution, blue short dash line) at a GC electrode. Potential: 0–1.5 V vs. Ag/AgCl and scan rate: 100 mV s<sup>-1</sup>.

sition which means that the complexes work as homogeneous catalysts for water oxidation under the neutral conditions.<sup>97</sup>

The catalytic current increases with the increasing concentration of the complex **2** (Fig. 8), demonstrating single-site copper catalysis. Furthermore, the addition of 1 mM Cu(NO<sub>3</sub>)<sub>2</sub> to 0.1 M phosphate buffer resulted in an immediate precipitation, and the resulting suspension/solution did not show any catalytic water oxidation activities (Fig. 8), indicating that the water oxidation was due to the complex rather than free Cu(II) ions in the solution. In addition, an inhibition experiment was performed to check the formation of Cu(II) ions from the decomposition of the catalyst in the solution. The ligand 2,2'-bipyridine (bpy) was used as the copper metal ion inhibitor during water oxidation catalysis. The addition of an excess amount of bpy to the solution using the complex **2** for catalysis did not result in any significant changes of catalytic activities (Fig. 8), confirming that no Cu<sup>2+</sup> ions were produced from the decomposition of the complex during the water oxidation reaction.

We performed bulk electrolysis experiments of a 0.5 mM solution of **1**, **2**, and **3** in 0.1 M phosphate buffer of pH 7.0 at 1.2 V for 2 h, then scanning electron microscopy (SEM) and energy-dispersive X-ray spectroscopy (EDS) were performed to check the morphology of the surface of the working electrode. SEM measurements after controlled potential electrolysis on a glassy carbon electrode confirmed that no heterogeneous film was deposited on the surface of the working electrode. The surface of the washed working electrode after controlled potential electrolysis at 1.2 V showed very similar features compared to the bare electrode (Fig. 9). EDS measurements also indicated no elemental metal and P except C on the surface of the working electrode. The element carbon in the EDS spectra was originated from the glassy carbon electrode (Fig. 10).

To check the stability of the catalysts during photochemical water oxidation and further follow up the formation of nano-

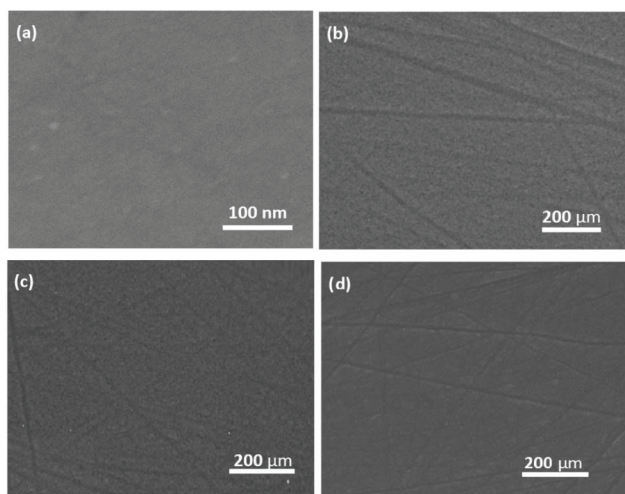


**Fig. 9** SEM images of the surface of the glassy carbon electrode; (a) before bulk electrolysis and after 2 hours of bulk electrolysis at 1.2 V (vs. Ag/AgCl) in 0.1 M phosphate buffer of pH 7.0 containing 0.5 mM (b) **1**, (c) **2**, and (d) **3**.

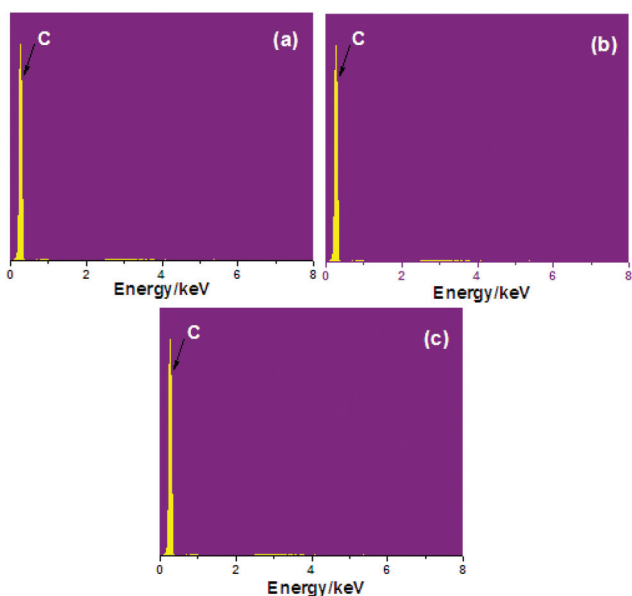


**Fig. 10** EDS histogram of the glassy carbon electrode after 2 h of bulk electrolysis at 1.2 V (vs. Ag/AgCl) in 0.1 M phosphate buffer of pH 7 containing 0.5 mM (a) **1**, (b) **2**, and (c) **3**.

particles, we performed the following experiment. A solution containing 0.2 mM catalyst, 2.4 mM  $[\text{Ru}(\text{bpy})_3]^{2+}$  and 5.0 mM  $\text{S}_2\text{O}_8^{2-}$  in a NaPi buffer (0.1 M) at pH 7.0 was irradiated under visible light for 60 min at room temperature. The solution mixture was analysed by ESI-MS and dynamic light scattering (DLS) measurements before and after 60 min of photolysis. The species observed in the electrospray ionization mass spectrum of the reaction mixture of **1** before photolysis were  $[\text{Ni}(\text{Slp})\text{H}]^+$  ( $m/z$ : 372.2023),  $[\text{Ru}(\text{bpy})_3]^{2+}$  ( $m/z$ : 285.141) and  $[\text{Ru}(\text{bpy})_3\text{Cl}]^+$  ( $m/z$ : 605.0018) (Fig. 11(a)). The ESI-MS spectrum

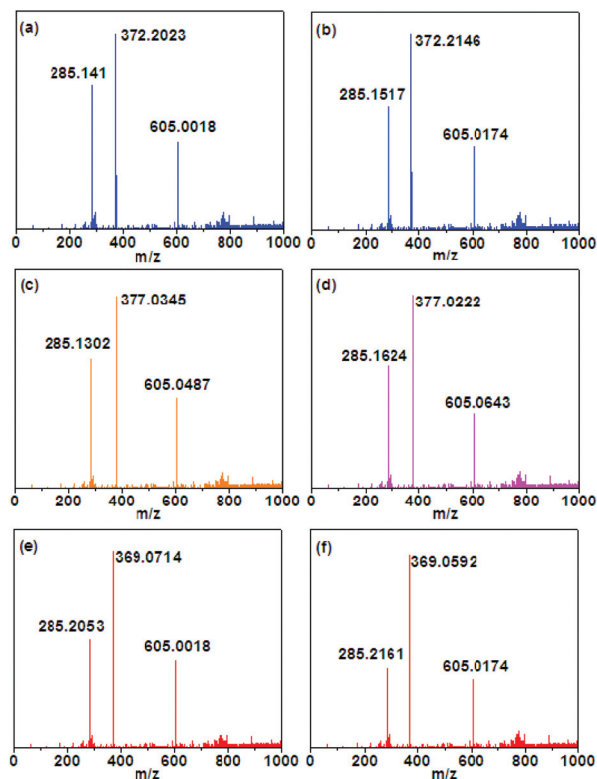


**Fig. 11** ESI-MS spectra of a solution containing 0.2 mM complex, 2.4 mM  $[\text{Ru}(\text{bpy})_3]^{2+}$  and 5.0 mM  $\text{Na}_2\text{S}_2\text{O}_8$  in a 0.1 M NaPi buffer of pH 7.0. Before photolysis: (a), (c), and (e) are for catalysts **1**, **2**, and **3**. After photolysis: (b), (d), and (f) are for catalysts **1**, **2**, and **3**. Irradiation with light ( $\lambda \geq 420$  nm) for 60 min at 23 °C.

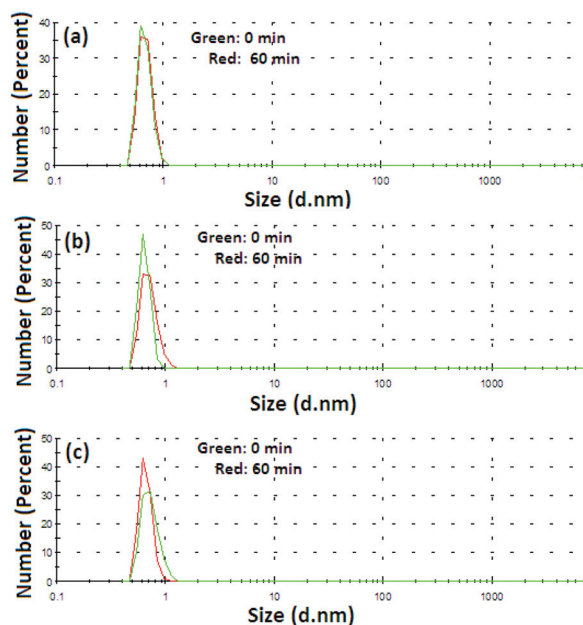


**Fig. 12** DLS measurements before and after 60 min of light irradiation of a solution containing 2.4 mM  $[\text{Ru}(\text{bpy})_3]^{2+}$ , 5.0 mM  $\text{S}_2\text{O}_8^{2-}$ , and 0.2 mM complex in 0.1 M NaPi buffer of pH 7.0. (a): Complex **1**, (b): complex **2** and (c): complex **3**.

(Fig. 11(c)) of the solution mixture of **2** showed the presence of  $\{[\text{Cu}(\text{Slp})\text{H}]^+\}$  ( $m/z$ : 377.0345),  $[\text{Ru}(\text{bpy})_3]^{2+}$  ( $m/z$ : 285.1302) and  $\{[\text{Ru}(\text{bpy})_3\text{Cl}]^+\}$  ( $m/z$ : 605.0487) before photolysis. The electro-spray mass spectrum of the solution mixture of **3** before photolysis (Fig. 11(e)) exhibited ions at mass-to-charge ratio ( $m/z$ ) of 369.0714, 285.2053, and 605.0018 matching the calculated values for the ions  $\{[\text{Mn}(\text{Slp})\text{H}]^+\}$ ,  $[\text{Ru}(\text{bpy})_3]^{2+}$  and  $\{[\text{Ru}(\text{bpy})_3\text{Cl}]^+\}$ , respectively. Consequently, the ESI-MS spectra of the solution mixture after photolysis (Fig. 11(b), (d), and (f)) were nearly identical to those of the solution mixture before photolysis; no other Co(II) species or the free salophen ligand was observed at  $m/z$  between 50 and 1000 in the ESI-MS, indicating that the catalysts were not decomposed during water oxidation catalysis.<sup>97</sup> Furthermore, dynamic light scattering (DLS) measurements of the reaction mixture before and after 60 min of light irradiation did not show any nanoparticle formation (Fig. 12).

## Conclusion

In summary, we have reported Earth-abundant metal-based catalysts **1**, **2**, and **3**, which are capable of oxidizing  $\text{H}_2\text{O}$  to  $\text{O}_2$  in the presence of  $\text{Ru}(\text{bpy})_3^{2+}$  as the photosensitizer and  $\text{Na}_2\text{S}_2\text{O}_8$  as the sacrificial electron acceptor at neutral pH. More importantly, all the catalysts were stable or homogeneous under the catalytic conditions, as examined by CV, SEM, EDX, ESI-MS, and DLS measurements. Our present study provides valuable insights into the development of robust water oxidation catalysts using Earth-abundant metals.

## Conflicts of interest

There are no conflicts to declare.

## Acknowledgements

The authors are grateful to the “State Key Lab of Advanced Technology for Materials Synthesis and Processing” for financial support. F. V. appreciates the financial support from Tomsk Polytechnic University Competitiveness Enhancement Program grant (VIU-2019). M. A. A. and C. I. E. thank the Chinese Scholarship Council (CSC) for the PhD grants 2013GXZ983 and 2013GXZ987.

## Notes and references

- N. S. Lewis and D. G. Nocera, *Proc. Natl. Acad. Sci. U. S. A.*, 2006, **103**, 15729–15735.
- H. Dau and I. Zaharieva, *Acc. Chem. Res.*, 2009, **42**, 1861–1870.
- Y. Umena, K. Kawakami, J.-R. Shen and N. Kamiya, *Nature*, 2011, **473**, 55–60.
- D. Gust, T. A. Moore and A. L. Moore, *Acc. Chem. Res.*, 2009, **42**, 1890–1898.
- P. E. Siegbahn, *Acc. Chem. Res.*, 2009, **42**, 1871–1880.
- A. Magnuson, M. Anderlund, O. Johansson, P. Lindblad, R. Lomoth, T. Polivka, S. Ott, K. Stensjö, S. Styring and V. Sundström, *Acc. Chem. Res.*, 2009, **42**, 1899–1909.
- J. P. McEvoy and G. W. Brudvig, *Chem. Rev.*, 2006, **106**, 4455–4483.
- L. Hammarström and S. Hammes-Schiffer, *Acc. Chem. Res.*, 2009, **42**, 1859–1860.
- L. Sun, L. Hammarström, B. Åkermark and S. Styring, *Chem. Soc. Rev.*, 2001, **30**, 36–49.
- H. Dau, C. Limberg, T. Reier, M. Risch, S. Roggan and P. Strasser, *ChemCatChem*, 2010, **2**, 724–761.
- P. D. Tran, V. Artero and M. Fontecave, *Energy Environ. Sci.*, 2010, **3**, 727–747.
- M. Yagi, A. Syouji, S. Yamada, M. Komi, H. Yamazaki and S. Tajima, *Photochem. Photobiol. Sci.*, 2009, **8**, 139–147.
- Y. Tamaura, M. Kojima, T. Sano, Y. Ueda, N. Hasegawa and M. Tsuji, *Int. J. Hydrogen Energy*, 1998, **23**, 1185–1191.
- R. Tagore, R. H. Crabtree and G. W. Brudvig, *Inorg. Chem.*, 2008, **47**, 1815–1823.
- G. C. Dismukes, R. Brimblecombe, G. A. Felton, R. S. Pryadun, J. E. Sheats, L. Spiccia and G. F. Swiegers, *Acc. Chem. Res.*, 2009, **42**, 1935–1943.
- M. M. Najafpour, S. Heidari, E. Amini, M. Khatamian, R. Carpentier and S. I. Allakhverdiev, *J. Photochem. Photobiol., B*, 2014, **133**, 124–139.
- S. W. Gersten, G. J. Samuels and T. J. Meyer, *J. Am. Chem. Soc.*, 1982, **104**, 4029–4030.
- A. Harriman, I. J. Pickering, J. M. Thomas and P. A. Christensen, *J. Chem. Soc., Faraday Trans. 1*, 1988, **84**, 2795–2806.
- J. J. Concepcion, J. W. Jurss, M. K. Brennaman, P. G. Hoertz, A. O. T. Patrocínio, N. Y. Murakami Iha, J. L. Templeton and T. J. Meyer, *Acc. Chem. Res.*, 2009, **42**, 1954–1965.
- J. F. Hull, D. Balcells, J. D. Blakemore, C. D. Incarvito, O. Eisenstein, G. W. Brudvig and R. H. Crabtree, *J. Am. Chem. Soc.*, 2009, **131**, 8730–8731.
- N. D. McDaniel, F. J. Coughlin, L. L. Tinker and S. Bernhard, *J. Am. Chem. Soc.*, 2008, **130**, 210–217.
- M. Graetzel, *Acc. Chem. Res.*, 1981, **14**, 376–384.
- W. Su, H. A. Younus, K. Zhou, Z. A. Khattak, S. Chaemcheun, C. Chen and F. Verpoort, *Catal. Sci. Technol.*, 2017, **7**, 387–395.
- H. B. Gray, *Nat. Chem.*, 2009, **1**, 7.
- H. Feizi, R. Bagheri, Z. Jagličić, J. P. Singh, K. H. Chae, Z. Song and M. M. Najafpour, *Dalton Trans.*, 2019, **48**, 547–557.
- M. Blasco-Ahicart, J. Soriano-López, J. J. Carbó, J. M. Poblet and J. Galan-Mascaros, *Nat. Chem.*, 2018, **10**, 24.
- H. A. Younus, N. Ahmad, A. H. Chughtai, M. Vandichel, M. Busch, K. Van Hecke, M. Yusubov, S. Song and F. Verpoort, *ChemSusChem*, 2017, **10**, 862–875.
- J. Lin, Q. Han and Y. Ding, *Chem. Rec.*, 2018, **18**, 1531–1547.

- 29 E. Pizzolato, M. Natali, B. Posocco, A. M. López, I. Bazzan, M. Di Valentin, P. Galloni, V. Conte, M. Bonchio and F. Scandola, *Chem. Commun.*, 2013, **49**, 9941–9943.
- 30 N. S. McCool, D. M. Robinson, J. E. Sheats and G. C. Dismukes, *J. Am. Chem. Soc.*, 2011, **133**, 11446–11449.
- 31 S. Berardi, G. La Ganga, M. Natali, I. Bazzan, F. Puntoriero, A. Sartorel, F. Scandola, S. Campagna and M. Bonchio, *J. Am. Chem. Soc.*, 2012, **134**, 11104–11107.
- 32 C.-F. Leung, S.-M. Ng, C.-C. Ko, W.-L. Man, J. Wu, L. Chen and T.-C. Lau, *Energy Environ. Sci.*, 2012, **5**, 7903–7907.
- 33 T. Nakazono, A. R. Parent and K. Sakai, *Chem. Commun.*, 2013, **49**, 6325–6327.
- 34 D. Wang and J. T. Groves, *Proc. Natl. Acad. Sci. U. S. A.*, 2013, **110**, 15579–15584.
- 35 D. J. Wasylenko, C. Ganesamoorthy, J. Borau-Garcia and C. P. Berlinguette, *Chem. Commun.*, 2011, **47**, 4249–4251.
- 36 D. K. Dogutan, R. McGuire Jr. and D. G. Nocera, *J. Am. Chem. Soc.*, 2011, **133**, 9178–9180.
- 37 H. Wang, Y. Lu, E. Mijangos and A. Thapper, *Chin. J. Chem.*, 2014, **32**, 467–473.
- 38 S. Fu, Y. Liu, Y. Ding, X. Du, F. Song, R. Xiang and B. Ma, *Chem. Commun.*, 2014, **50**, 2167–2169.
- 39 D. Hong, J. Jung, J. Park, Y. Yamada, T. Suenobu, Y.-M. Lee, W. Nam and S. Fukuzumi, *Energy Environ. Sci.*, 2012, **5**, 7606–7616.
- 40 M. Dincă, Y. Surendranath and D. G. Nocera, *Proc. Natl. Acad. Sci. U. S. A.*, 2010, **107**, 10337–10341.
- 41 D. K. Bediako, B. Lassalle-Kaiser, Y. Surendranath, J. Yano, V. K. Yachandra and D. G. Nocera, *J. Am. Chem. Soc.*, 2012, **134**, 6801–6809.
- 42 G. Chen, L. Chen, S. M. Ng and T. C. Lau, *ChemSusChem*, 2014, **7**, 127–134.
- 43 X. Yu, T. Hua, X. Liu, Z. Yan, P. Xu and P. Du, *ACS Appl. Mater. Interfaces*, 2014, **6**, 15395–15402.
- 44 A. Singh, S. L. Chang, R. K. Hocking, U. Bach and L. Spiccia, *Energy Environ. Sci.*, 2013, **6**, 579–586.
- 45 A. Singh, S. L. Chang, R. K. Hocking, U. Bach and L. Spiccia, *Catal. Sci. Technol.*, 2013, **3**, 1725–1732.
- 46 Z. Chen and T. J. Meyer, *Angew. Chem.*, 2013, **125**, 728–731.
- 47 M.-T. Zhang, Z. Chen, P. Kang and T. J. Meyer, *J. Am. Chem. Soc.*, 2013, **135**, 2048–2051.
- 48 X. Liu, H. Jia, Z. Sun, H. Chen, P. Xu and P. Du, *Electrochem. Commun.*, 2014, **46**, 1–4.
- 49 W. C. Ellis, N. D. McDaniel, S. Bernhard and T. J. Collins, *J. Am. Chem. Soc.*, 2010, **132**, 10990–10991.
- 50 J. L. Fillol, Z. Codolà, I. Garcia-Bosch, L. Gómez, J. J. Pla and M. Costas, *Nat. Chem.*, 2011, **3**, 807–813.
- 51 D. Hong, S. Mandal, Y. Yamada, Y.-M. Lee, W. Nam, A. Llobet and S. Fukuzumi, *Inorg. Chem.*, 2013, **52**, 9522–9531.
- 52 M. M. Najafpour, F. Ebrahimi, R. Safdari, M. Z. Ghobadi, M. Tavahodi and P. Rafeighi, *Dalton Trans.*, 2015, **44**, 15435–15440.
- 53 W.-B. Yu, Q.-Y. He, X.-F. Ma, H.-T. Shi and X. Wei, *Dalton Trans.*, 2015, **44**, 351–358.
- 54 M. M. Najafpour, R. Safdari, F. Ebrahimi, P. Rafeighi and R. Bagheri, *Dalton Trans.*, 2016, **45**, 2618–2623.
- 55 M. A. Asraf, H. A. Younus, C. I. Ezugwua and A. Mehta, *Catal. Sci. Technol.*, 2016, **6**, 4271–4282.
- 56 M. A. Asraf, H. A. Younus, M. S. Yusubov and F. Verpoort, *Catal. Sci. Technol.*, 2015, **5**, 4901–4925.
- 57 Y. Liu, Y. Han, Z. Zhang, W. Zhang, W. Lai, Y. Wang and R. Cao, *Chem. Sci.*, 2019, **10**, 2613–2622.
- 58 S. I. Shylin, M. V. Pavliuk, L. D'Amario, F. Mamedov, J. Sá, G. Berggren and I. O. Fritsky, *Chem. Commun.*, 2019, **55**, 3335–3338.
- 59 S. Fukuzumi, Y.-M. Lee and W. Nam, *Dalton Trans.*, 2019, **48**, 779–798.
- 60 S. Fukuzumi and D. Hong, *Eur. J. Inorg. Chem.*, 2014, **2014**, 645–659.
- 61 F. Song, Y. Ding, B. Ma, C. Wang, Q. Wang, X. Du, S. Fu and J. Song, *Energy Environ. Sci.*, 2013, **6**, 1170–1184.
- 62 J. Lin, B. Ma, M. Chen and Y. Ding, *Chin. J. Catal.*, 2018, **39**, 463–471.
- 63 D. A. Atwood and M. J. Harvey, *Chem. Rev.*, 2001, **101**, 37–52.
- 64 P. G. Cozzi, *Chem. Soc. Rev.*, 2004, **33**, 410–421.
- 65 C. Baleizao and H. Garcia, *Chem. Rev.*, 2006, **106**, 3987–4043.
- 66 H. Chen, Z. Sun, X. Liu, A. Han and P. Du, *J. Phys. Chem. C*, 2015, **119**(17), 8998–9004.
- 67 M. W. Kanan and D. G. Nocera, *Science*, 2008, **321**, 1072–1075.
- 68 S. M. Barnett, K. I. Goldberg and J. M. Mayer, *Nat. Chem.*, 2012, **4**, 498–502.
- 69 M. L. Rigsby, S. Mandal, W. Nam, L. C. Spencer, A. Llobet and S. S. Stahl, *Chem. Sci.*, 2012, **3**, 3058–3062.
- 70 T. Zhang, C. Wang, S. Liu, J.-L. Wang and W. Lin, *J. Am. Chem. Soc.*, 2013, **136**, 273–281.
- 71 C. Panda, J. Debgupta, D. Díaz Díaz, K. K. Singh, S. Sen Gupta and B. B. Dhar, *J. Am. Chem. Soc.*, 2014, **136**, 12273–12282.
- 72 S. Pattanayak, D. R. Chowdhury, B. Garai, K. K. Singh, A. Paul, B. B. Dhar and S. S. Gupta, *Chem. – Eur. J.*, 2017, **23**, 3414–3424.
- 73 A. A. Khandar, B. Shaabani, F. Belaj and A. Bakhtiari, *Inorg. Chim. Acta*, 2007, **360**, 3255–3264.
- 74 L. F. Lindoy, W. E. Moody and D. Taylor, *Inorg. Chem.*, 1977, **16**, 1962–1968.
- 75 M. Sönmez, M. R. Bayram and M. Çelebi, *J. Coord. Chem.*, 2009, **62**, 2728–2735.
- 76 T. Chen and C. Cai, *Synth. Commun.*, 2015, **45**, 1334–1341.
- 77 K. Srinivasan, P. Michaud and J. K. Kochi, *J. Am. Chem. Soc.*, 1986, **108**, 2309–2320.
- 78 A. Sánchez-Méndez, J. M. Benito, E. de Jesús, F. J. de la Mata, J. C. Flores, R. Gómez and P. Gómez-Sal, *Dalton Trans.*, 2006, 5379–5389.
- 79 R. S. Drago and W. B. S. Company, *Physical methods in chemistry*, W.B. Saunders Company, Philadelphia, 1977.
- 80 I. Bertini, P. Turano and A. J. Vila, *Chem. Rev.*, 1993, **93**, 2833–2932.

- 81 E. Szajna, P. Dobrowolski, A. L. Fuller, A. M. Arif and L. M. Berreau, *Inorg. Chem.*, 2004, **43**, 3988–3997.
- 82 C. Belle, C. Bougault, M.-T. Averbuch, A. Durif, J.-L. Pierre, J.-M. Latour and L. Le Pape, *J. Am. Chem. Soc.*, 2001, **123**, 8053–8066.
- 83 R. C. Holz, E. A. Evdokimov and F. T. Gobena, *Inorg. Chem.*, 1996, **35**, 3808–3814.
- 84 A. B. Tossi and H. Görner, *J. Photochem. Photobiol., B*, 1993, **17**, 115–125.
- 85 K. Henbest, P. Douglas, M. S. Garley and A. Mills, *J. Photochem. Photobiol., A*, 1994, **80**, 299–305.
- 86 X. Zhou, F. Li, H. Li, B. Zhang, F. Yu and L. Sun, *ChemSusChem*, 2014, **7**, 2453–2456.
- 87 J. J. Stracke and R. G. Finke, *ACS Catal.*, 2014, **4**, 909–933.
- 88 G. Zhu, Y. V. Geletii, P. Kögerler, H. Schilder, J. Song, S. Lense, C. Zhao, K. I. Hardcastle, D. G. Musaev and C. L. Hill, *Dalton Trans.*, 2012, **41**, 2084–2090.
- 89 T. A. Betley, Q. Wu, T. Van Voorhis and D. G. Nocera, *Inorg. Chem.*, 2008, **47**, 1849–1861.
- 90 M. H. V. Huynh and T. J. Meyer, *Chem. Rev.*, 2007, **107**, 5004–5064.
- 91 J. J. Concepcion, J. W. Jurss, J. L. Templeton and T. J. Meyer, *J. Am. Chem. Soc.*, 2008, **130**, 16462–16463.
- 92 H.-W. Tseng, R. Zong, J. T. Muckerman and R. Thummel, *Inorg. Chem.*, 2008, **47**, 11763–11773.
- 93 Y. Han, Y. Wu, W. Lai and R. Cao, *Inorg. Chem.*, 2015, **54**, 5604–5613.
- 94 L. Wang, L. Duan, R. B. Ambre, Q. Daniel, H. Chen, J. Sun, B. Das, A. Thapper, J. Uhlig and P. Dinér, *J. Catal.*, 2016, **335**, 72–78.
- 95 D. R. Weinberg, C. J. Gagliardi, J. F. Hull, C. F. Murphy, C. A. Kent, B. C. Westlake, A. Paul, D. H. Ess, D. G. McCafferty and T. J. Meyer, *Chem. Rev.*, 2012, **112**, 4016–4093.
- 96 D. W. Shaffer, Y. Xie and J. J. Concepcion, *Chem. Soc. Rev.*, 2017, **46**, 6170–6193.
- 97 M. Zhang, M.-T. Zhang, C. Hou, Z.-F. Ke and T.-B. Lu, *Angew. Chem., Int. Ed.*, 2014, **53**, 13042–13048.